JACS
JOURNAL OF THE AMERICAN CHEMICAL SOCIETY
Article
pubs.acs.org/JACS

Carbon Dots as Versatile Photosensitizers for Solar-Driven Catalysis with Redox Enzymes

Georgina A. M. Hutton,[†] Bertrand Reuillard,[†] Benjamin C. M. Martindale,[†] Christine A. Caputo,[†,§] Colin W. J. Lockwood,[‡] Julea N. Butt,[‡] and Erwin Reisner*[,†]

[†]Department of Chemistry, University of Cambridge, Lensfield Road, Cambridge CB2 1EW, U.K.
[‡]School of Chemistry and School of Biological Sciences, University of East Anglia, Norwich Research Park, Norwich NR4 7TJ, U.K.

Supporting Information

ABSTRACT: Light-driven enzymatic catalysis is enabled by the productive coupling of a protein to a photosensitizer. Photosensitizers used in such hybrid systems are typically costly, toxic, and/or fragile, with limited chemical versatility. Carbon dots (CDs) are low-cost, nanosized light-harvesters that are attractive photosensitizers for biological systems as they are water-soluble, photostable, nontoxic, and their surface chemistry can be easily modified. We demonstrate here that CDs act as excellent light-absorbers in two semibiological photosynthetic systems utilizing either a fumarate reductase (FccA) for the solar-driven hydrogenation of fumarate to succinate or a hydrogenase (H_2ase) for reduction of protons to H_2. The tunable surface chemistry of the CDs was exploited to synthesize positively charged ammonium-terminated CDs (CD-$NHMe_2^+$), which were capable of transferring photoexcited electrons directly to the negatively charged enzymes with high efficiency and stability. Enzyme-based turnover numbers of 6000 mol succinate (mol FccA)$^{-1}$ and 43,000 mol H_2 (mol H_2ase)$^{-1}$ were reached after 24 h. Negatively charged carboxylate-terminated CDs (CD-CO_2^-) displayed little or no activity, and the electrostatic interactions at the CD−enzyme interface were determined to be essential to the high photocatalytic activity observed with CD-$NHMe_2^+$. The modular surface chemistry of CDs together with their photostability and aqueous solubility make CDs versatile photosensitizers for redox enzymes with great scope for their utilization in photobiocatalysis.

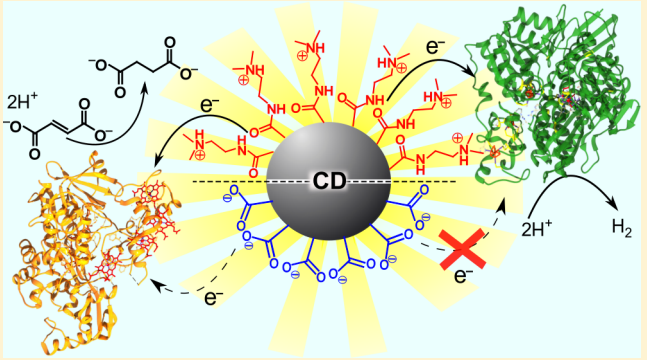

INTRODUCTION

Natural photosynthesis inspires the design of synthetic systems for the conversion of solar energy into chemical fuels, i.e., artificial photosynthesis.[1−3] This approach has spurred the development of semibiological systems that couple a synthetic light harvesting unit to an isolated enzyme[4−8] or organism.[9−13] Such systems combine the efficient light-harvesting properties of synthetic materials with the high selectivity and rates of biological catalysts.[9,13]

Semibiological systems require a profound understanding of the mechanisms of interfacial electron transfer between the abiotic and biotic components. Significant work has focused on integrating isolated redox enzymes into proof-of-principle photocatalytic and electrochemical systems for solar fuel synthesis.[4,6,14−16] Such systems allow enzymatic redox processes to be decoupled from their biological metabolism and to be studied in isolation, providing insights into the interfacial electron transfer processes between the protein and an electrode or dye.[17,18] Hydrogenases (H_2ases) are of particular interest for use in semibiological solar fuel systems as they are model precious metal free proton reduction electrocatalysts, capable of operating with turnover frequencies comparable to that of Pt.[19−22] The light-harvesting ability of natural photosystems has been coupled to H_2 production by H_2ase in vitro via H_2ase-photosystem I protein conjugates,[23,24] or by the electrochemical wiring of H_2ase to photosystems I[25] and II.[15] Approaches employing synthetic light absorbers include immobilizing H_2ase onto silicon photoelectrodes[6,8] as well as utilizing H_2ase in homogeneous and semiheterogeneous photocatalytic systems using organic and inorganic molecular dyes[26−29] or semiconductor particles such as dye-sensitized TiO_2,[30,31] graphitic carbon nitride,[32] Cd chalcogenides,[33−35] and In_2S_3.[36]

Beyond the use of enzymes as benchmark catalysts for solar fuel production, enzyme-driven catalysis is also well established for achieving complex organic redox transformations with high selectivity.[37−39] Often, however, stoichiometric equivalents of expensive reducing cofactors such as NADPH are required to mediate the enzymatic reaction.[37,40,41] As such, there is scope for the integration of enzymes into biohybrid photocatalytic schemes that utilize solar energy to drive NADPH recycling, or to directly reduce the enzyme, eliminating the need for the cofactor altogether.[38,40,42,43] Only a small number of mediator-

Received: September 27, 2016
Published: November 28, 2016

DOI: 10.1021/jacs.6b10146
J. Am. Chem. Soc. XXXX, XXX, XXX−XXX

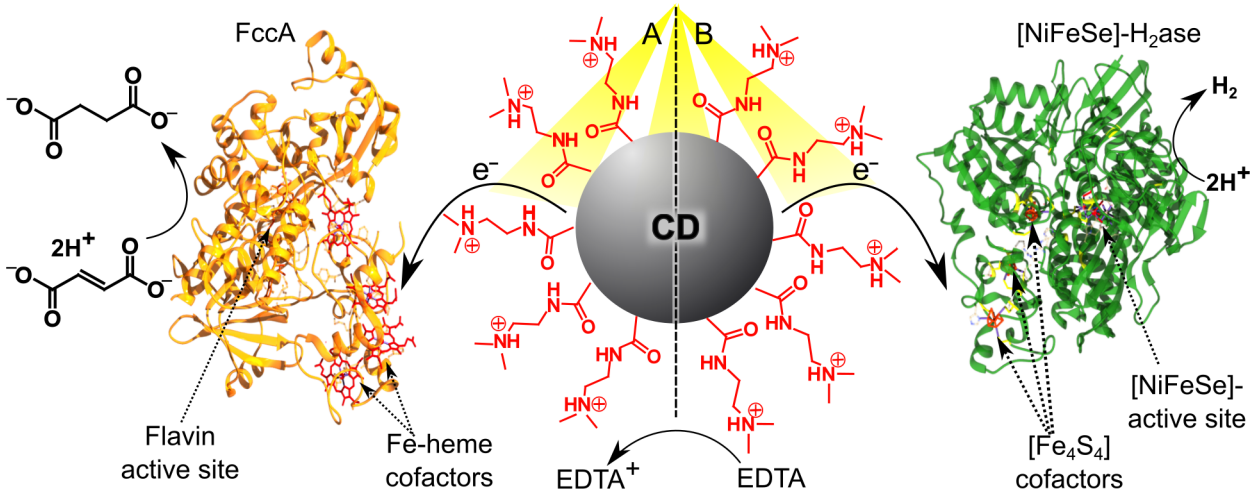

Figure 1. Representations of the two independent photocatalytic systems studied in this work: photoexcited CDs transfer electrons to a fumarate reductase (FccA; system A) or a [NiFeSe]-hydrogenase (H_2ase; system B) for the reduction of fumarate to succinate and protons to H_2, respectively; EDTA acts as a sacrificial hole scavenger. The location of the active site in each enzyme is labeled in addition to the Fe-heme and $[Fe_4S_4]$ cofactors for FccA and H_2ase, respectively.

free dye−enzyme hybrids have been reported to photocatalyze organic chemical transformations, however, with the photosensitizers typically being limited to (dye-sensitized) TiO_2 nanoparticles[44] and organic[11] and ruthenium tris-2,2′-bipyridine dyes.[29,45]

Despite the widespread use of dyes with enzymes for photocatalysis as well as in the study of electron transfer in dye−protein[46] and dye−nucleic acid[47] assemblies, there remain a limited number of suitable photosensitizers available. Photosystems[23,24] and abiotic molecular dyes[11,26] suffer from fragility. Molecular dyes can also be time-consuming to synthesize and are often expensive, particularly those containing precious metals.[44,48] Semiconductor particles often have good stability, but common disadvantages include poor interfacial interaction with the redox partner (graphitic carbon nitrides),[32] toxicity (Cd chalcogenides),[33−35] low elemental abundance (Cd, Te, and In),[35,36,49] and poor aqueous dispersibility (TiO_2 and carbon nitrides).[31,32,44,48] Most light absorbers are also challenging to chemically modify and can create highly oxidizing or reducing species that are detrimental to the lifetime of a biomacromolecule.[44] Thus, there remains a need for the development of photosensitizers that are capable of interfacing efficiently with biological materials.

In this study, carbon dots (CDs) are established as versatile, low-cost, stable and efficient photosensitizers for photobiocatalysis (Figure 1). First, a system utilizing CDs and fumarate reductase (FccA), a flavoenzyme from *Shewanella oneidensis* MR-1, is presented for the photoconversion of fumarate to succinate: a model system for enzyme-driven C=C bond hydrogenation, an important redox transformation in organic chemistry.[41,43,44] The study of this photocatalytic hybrid system was complemented by optical spectroscopy, monitoring the photoreduction of the four Fe^{3+}-heme cofactors in FccA.[50,51] Finally, solar H_2 generation is shown using CDs and a [NiFeSe]-H_2ase from *Desulfomicrobium baculatum* (*Dmb*). Taking advantage of the tunable CD surface chemistry, we have synthesized negatively and positively charged CDs and demonstrate that only the cationic CDs are capable of efficient photoelectron transfer to the negatively charged proteins, due to a favorable interfacial interaction.

RESULTS AND DISCUSSION

Synthesis and Characterization of CDs. CDs are photoluminescent carbon nanomaterials that have promising light harvesting and electron transfer capabilities for applications in photocatalysis.[52−54] We have recently demonstrated CDs to be stable and efficient photosensitizers in a homogeneous photocatalytic H_2 generation scheme using a synthetic molecular Ni catalyst.[55,56] Although CD−protein assemblies have been studied previously,[57−62] they have not been reported for the light-driven synthesis of chemical products, i.e., artificial photosynthesis.

The solubility in water and biocompatibility of CDs has already led to significant interest in CDs for nanotherapeutic,[63,64] bioimaging,[65,66] and biochemical sensing[67−69] applications. Furthermore, CD surfaces are typically carboxylic acid terminated or amine-terminated and can be readily manipulated. This provides a versatile platform to design and tune the interface between the CDs and a protein, which may be crucial to optimize electron transfer efficiency.[70] Carboxylic acid terminated and amine-terminated CDs are expected to be anionic and cationic at pH neutral conditions, respectively, and are therefore well suited to probe the effect of electrostatic interactions with a redox partner.

The carboxylic acid terminated and amine-terminated CDs used in this study were prepared as shown in Scheme 1, with experimental and characterization details described in the Experimental Section. Carboxylic acid capped CDs (CD-CO_2H) were synthesized by the thermal decomposition of citric acid as previously reported.[55,71] The carboxylic acid surface groups were then selectively modified by treatment with thionyl chloride to yield acyl chloride capped CDs (CD-COCl).[72,73] CD-COCl can be isolated by evaporation of the excess thionyl chloride and are readily soluble in polar organic solvents such as tetrahydrofuran, acetonitrile, and acetone. The high reactivity of the acyl chloride group and absence of nonvolatile byproducts provide an adaptable route to tunable surface chemistry without the need for elaborate purification procedures.[73] Stirring CD-COCl with the nucleophile *N*,*N*-dimethylethylenediamine (DMEN) at room temperature followed by evaporation of the residual DMEN results in

DOI: 10.1021/jacs.6b10146
J. Am. Chem. Soc. XXXX, XXX, XXX−XXX

Scheme 1. Synthesis and Surface Functionalization of CDs[a]

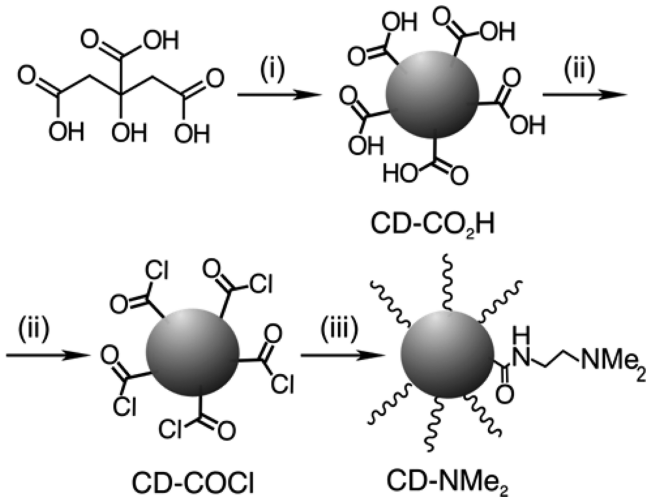

[a](i) 180 °C, 40 h; (ii) $SOCl_2$ (neat), 80 °C, 1 h; (iii) DMEN (neat), 25 °C, 3 h.

tertiary amine capped CDs (CD-NMe_2). The tertiary amine was chosen to avoid cross-linking between particles or adjacent surface groups.

The chemical modification of the CD-CO_2H carboxylic acid surface groups was monitored by attenuated total reflectance Fourier transform infrared spectroscopy (ATR FT-IR; Figure 2). As expected, a clear shift in the C═O stretching frequency is observed, from $\tilde{\nu}$ = 1701 cm^{-1} (CD-CO_2H) to 1760 cm^{-1} (CD-COCl) and then to 1654 cm^{-1} (CD-NMe_2).[73] The amide carbonyl stretch (1654 cm^{-1}) in CD-NMe_2 with a corresponding amide N−H bending mode ($\tilde{\nu}$ = 1546 cm^{-1}) confirms that DMEN has reacted with CD-COCl and is covalently bound to the CD surface. Further features of the DMEN reagent are also observed on the CD-NMe_2 surface, such as the C−H stretching ($\tilde{\nu}$ = 2948, 2865, 2827, and 2770 cm^{-1}) and bending ($\tilde{\nu}$ = 1460 cm^{-1}) modes. The small peak at $\tilde{\nu}$ = 1700 cm^{-1} in CD-NMe_2 suggests that some acyl chloride residues from CD-COCl have been hydrolyzed possibly by residual water in the DMEN reagent. The broad signal at $\tilde{\nu}$ = 3500−3260 cm^{-1} in CD-NMe_2 is most likely largely due to absorbed water given that the sample is very hygroscopic.

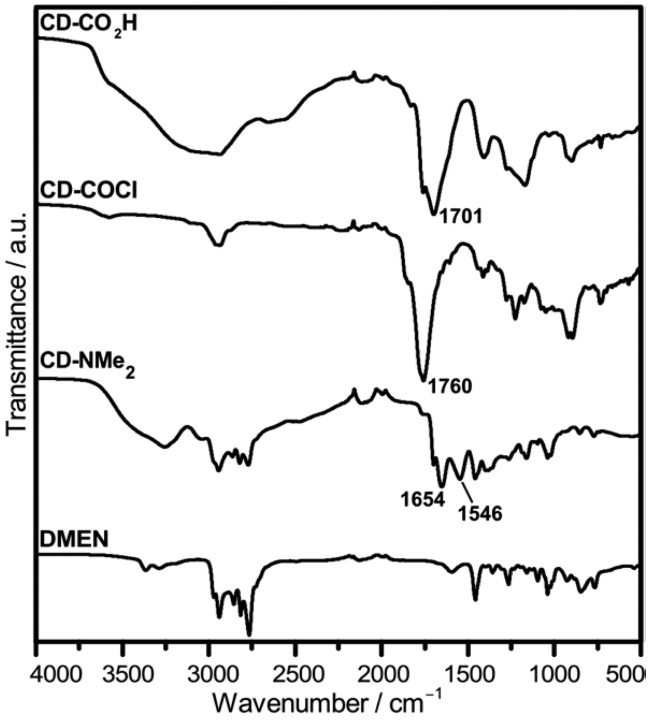

Figure 2. ATR FT-IR spectra of CD-CO_2H, CD-COCl, CD-NMe_2, and DMEN.

The surface functionalization of CD-NMe_2 was further studied by ^1H NMR spectroscopy, shown in Figure S1. Two sets of triplets and a singlet were observed, which can be assigned to the ethylene and methyl protons of the surface functional groups, respectively. No proton signals from DMEN or the protonated DMEN salt were observed in the final CD-NMe_2 product, which supports that all excess amine reagent was removed during the workup process.

Transmission electron microscopy (TEM) and UV−visible (UV−vis) absorption spectroscopy indicate that the bulk physical properties of the CDs are not significantly altered during the surface functionalization procedure. TEM analysis showed an average particle size of 6.4 nm ± 1.2 nm for CD-NMe_2 (see Figure S2), which is similar to CD-CO_2H.[55] The UV−vis spectrum of CD-NMe_2 in aqueous solution shows a broad absorption typical of CDs, assigned to various $\pi-\pi^*$ (C═C) and $n-\pi^*$ (C═O) absorptions (Figure S3).[53] The absorption onset of CD-NMe_2 is slightly shifted to longer wavelengths compared to CD-CO_2H, which is consistent with previous reports of amide-functionalized CDs.[72]

Zeta potential (ζ) measurements were carried out to study the surface charge of the CDs (Figure S4). The isoelectric point (I_p) for CD-CO_2H was determined to be approximately 1, whereas the I_p for CD-NMe_2 was approximately 9. The surfaces of CD-CO_2H and CD-NMe_2 are therefore negatively (ζ = −17 ± 5 mV) and positively charged (ζ = +17 ± 1 mV) under the photocatalysis conditions employed in this study (pH 6, see below). We therefore denote the CDs as CD-CO_2^- and CD-$NHMe_2^+$ to accurately describe their ionic character in the photocatalysis sections below.

Photoreduction of FccA with CDs. FccA, a flavoenzyme c_3 from *Shewanella oneidensis* MR-1, catalyzes the reduction of fumarate to succinate. FccA is an ideal candidate to study electron transfer from CDs due to the positive redox potential for fumarate reduction ($E^{\circ\prime}$ = 0.03 V vs SHE at pH 7) and low FccA overpotential (80 mV at pH 7).[44,74] Fumarate is reduced to succinate at the flavin active site by the transfer of one hydride from the flavin and one proton from a nearby arginine residue.[74−76] The electron transport chain from the surface to the flavin active site consists of four *c*-type Fe-heme groups, as shown in Figure 1. The UV-vis absorption spectrum of these Fe^{3+}-heme cofactors is characterized by an intense Soret band at 408 nm as well as a broad feature from 500 to 600 nm. Upon reduction of the protein, new bands appear at 419, 523, and 552 nm, which can be assigned to the Fe^{2+}-heme cofactors.[50,51]

The characteristic absorption of the Fe^{2+}-heme cofactors thus provides a useful spectroscopic handle to study the ability of CDs to photoreduce FccA using UV−vis absorption spectroscopy. An aqueous solution containing the buffer and sacrificial electron donor ethylenediaminetetraacetic acid (EDTA; 0.1 M, pH 6) was selected as the reaction medium, as EDTA has previously been shown to be the optimized electron donor for CDs[55] and the slightly acidic pH is within the ideal pH range for FccA activity (pH 5−8).[50,51,74]

DOI: 10.1021/jacs.6b10146
J. Am. Chem. Soc. XXXX, XXX, XXX−XXX

Figure 3 shows the time-resolved UV−vis spectra of a solution containing FccA (0.33 μM) and CD-NHMe$_2^+$ (1 mg mL^{-1}) in aqueous EDTA solution under simulated solar light irradiation (AM 1.5G, 100 mW cm^{-2}) at 25 °C in the absence of fumarate (see Figure S5 for CD-CO$_2^-$). Upon irradiation, the characteristic Fe^{2+}-heme absorption bands are observed to appear and reach a steady state after approximately 8 min (Figure S5).

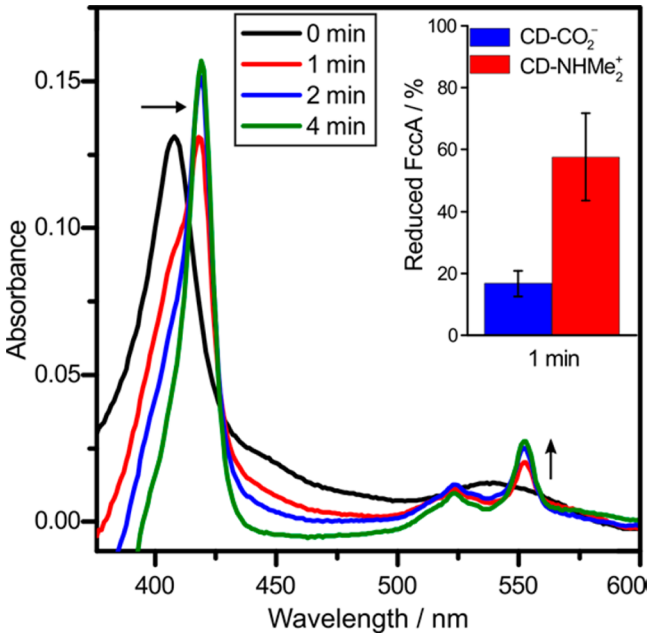

Figure 3. UV−visible absorption spectra of FccA (0.33 μM) in the presence of CD-NHMe$_2^+$ (1 mg mL^{-1}) and EDTA (0.1 M, pH 6) recorded before and after 1, 2, and 4 min illumination with simulated solar light irradiation (AM 1.5G, 100 mW cm^{-2}) at 25 °C. The inset shows the fraction of FccA reduced after 1 min using CD-CO$_2^-$ and CD-NHMe$_2^+$, calculated from the increase of the peak at 523 nm. The cuvette path length was 1 cm.

Although both CD-NHMe$_2^+$ and CD-CO$_2^-$ are capable of reducing FccA over several minutes, CD-NHMe$_2^+$ photoreduces FccA at a substantially higher rate, with 60% of the heme units reduced after 1 min compared to 20% when using CD-CO$_2^-$ (see inset Figure 3). This difference in the initial rate of FccA reduction under nonturnover conditions becomes significant in the study of the CD-FccA systems during photocatalysis in the presence of a substrate (see below).

Solar-Driven Fumarate Reduction with CDs and FccA. The CD-FccA system was subsequently studied under simulated solar light irradiation in the presence of fumarate, and the photogeneration of succinate was monitored by ^{1}H NMR spectroscopy (Figure 4, Table S1). The photocatalytic experiments were set up by dissolving CDs (1 mg), FccA (0.22 nmol), and fumarate (10 mM) in an EDTA solution prepared in D$_2$O (0.1 M, pD 6.4,[77] 1 mL; see Experimental Section for details). The vials were then purged with N$_2$ and irradiated by a solar light simulator (AM 1.5G) at 100 mW cm^{-2} (1 sun). Aliquots of the photocatalysis mixture (0.2 mL) were analyzed directly by ^{1}H NMR after 2, 4, 8, and 24 h. The turnover number (TON) for succinate production per FccA (TON$_{FccA}$) was determined by the integral ratio of the ^{1}H NMR peaks corresponding to fumarate (6.44 ppm) and succinate (2.33 ppm).[44] Representative ^{1}H NMR spectra are shown in Figure S6.

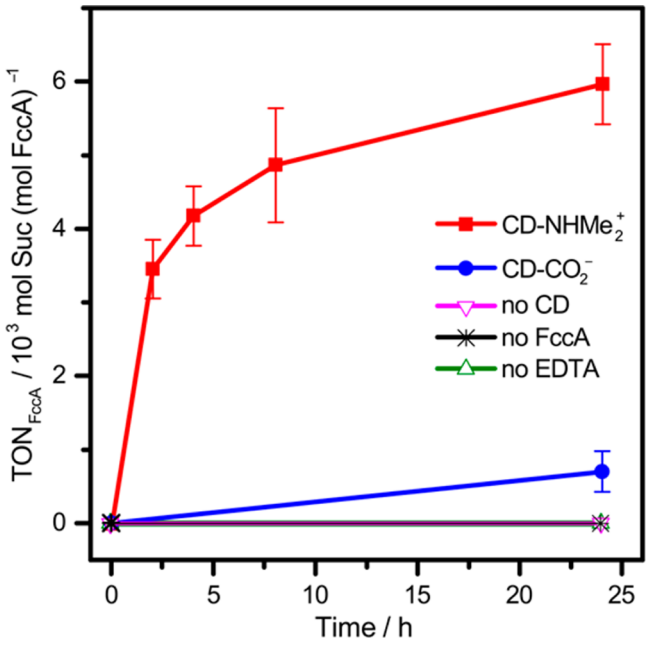

Figure 4. Succinate production using CDs (1 mg) with FccA (0.22 nmol) in the presence of fumarate (10 mM) and EDTA (0.1 M) in D$_2$O (1 mL, pD 6.4) under simulated solar light irradiation (AM 1.5G, 100 mW cm^{-2}) at 25 °C. Control experiments without CDs, FccA, or EDTA (the latter two with CD-NHMe$_2^+$) are also shown. Solid lines have been added to guide the eye.

Figure 4 shows that while both CDs are capable of direct electron transfer to FccA, the photoreduction of fumarate is significantly enhanced with CD-NHMe$_2^+$ compared to CD-CO$_2^-$, consistent with the higher rate of Fe^{3+}-heme reduction observed spectroscopically. Control experiments in the absence of CDs, FccA, or EDTA showed no succinate production. The similar bulk physical properties of the CDs suggest that the markedly different performance in photocatalytic succinate production is due to the different surface charges of the CDs, resulting in different interfacial interactions with FccA (see discussion in CD−Enzyme Interface).

The CD-NHMe$_2^+$-FccA system operated at an initial enzyme-based turnover frequency (TOF$_{FccA}$) of 1.7 ± 0.2 × 10^3 mol succinate (mol FccA)$^{-1}$ h^{-1} and remained photoactive for at least 24 h, after which time a TON$_{FccA}$ of 6.0 ± 0.6 × 10^3 mol succinate (mol FccA)$^{-1}$ had been reached (Figure 4, Table S1). The decrease in rate observed after 2 h is attributed to enzyme degradation rather than photoinstability of the CDs (see CD−Enzyme Interface). Previously FccA has only been studied under photocatalysis conditions using Ru dye-sensitized TiO$_2$ nanoparticles as the photosensitizer, achieving a comparable TON$_{FccA}$ of 5.8 × 10^3 with activity ceasing after 4 h.[44]

Solar-Driven H_2 Production with CDs and H_2ase. Having established that the CDs are capable of direct electron transfer to FccA in an aqueous sacrificial photocatalysis system, we investigated the CDs in a solar H$_2$ production system with *Dmb* [NiFeSe]-H$_2$ase (Figure 1). *Dmb* [NiFeSe]-H$_2$ase was chosen as it is well established for use in homogeneous and semiheterogeneous photocatalytic H$_2$ generation systems.[78] [NiFeSe]-H$_2$ase is a subclass of [NiFe]-H$_2$ases with a selenocysteine residue coordinated to Ni at the active site

DOI: 10.1021/jacs.6b10146
J. Am. Chem. Soc. XXXX, XXX, XXX−XXX

instead of a cysteine residue.[79] Three [Fe_4S_4]-clusters form the electron transport chain to the active site, as shown in Figure 1. [NiFeSe]-H_2ases are known for their good H_2 evolution activity ($E^{\circ\prime}$ (H^+/H_2) = −0.41 vs SHE at pH 7), resistance to O_2, and low product inhibition.[79,80]

For the CD-H_2ase systems studied here, EDTA was again chosen as sacrificial electron donor and pH 6 as the optimal pH for H_2ase activity.[48] A ratio of H_2ase (50 pmol) to CD (10 mg) was selected after optimization of the CD loading for the highest TON_{H2ase} after 24 h; the H_2ase loading was kept at 50 pmol to aid comparison to comparable systems with different light absorbers (see Figure S7).[31,32] The photocatalytic systems were typically assembled by dissolving CDs (10 mg) and H_2ase (50 pmol) in a degassed aqueous solution of EDTA (0.1 M, pH 6, 3 mL) in a borosilicate glass vessel of total volume 7.74 mL. The photoreactor was purged with N_2 containing 2% CH_4 as an internal gas chromatography (GC) standard and tightly sealed. The vials were then irradiated (AM 1.5G, 100 mW cm^{-2}), and the headspace gas was periodically monitored by GC.

Figure 5 shows the solar H_2 production activity of H_2ase using CD-$NHMe_2^+$ and CD-CO_2^- as photosensitizers. Similar

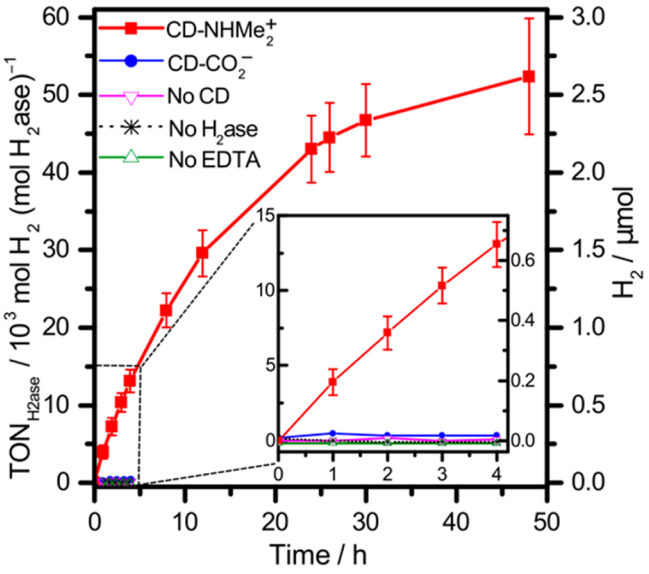

Figure 5. H_2 production using CD-$NHMe_2^+$ and CD-CO_2^- (10 mg) with *Dmb* [NiFeSe]-H_2ase (50 pmol) in aqueous EDTA solution (0.1 M, pH 6) during AM 1.5G irradiation (100 mW cm^{-2}) at 25 °C. Control experiments without CDs, H_2ase, or EDTA (the latter two with CD-$NHMe_2^+$) are also shown.

to their behavior with FccA, the CD surface has a significant impact on the photo-H_2 production (see discussion below). Negligible H_2 generation was observed with CD-CO_2^-, whereas CD-$NHMe_2^+$ showed high photoactivity with a TOF_{H2ase} of 3.9 ± 0.9 × 10^3 mol H_2 (mol H_2ase)$^{-1}$ h^{-1} and long-term H_2 production, reaching a TON_{H2ase} of 52 ± 8 × 10^3 mol H_2 (mol H_2ase)$^{-1}$ after 48 h (Figure 5, Table S2). The performance of this CD-$NHMe_2^+$-H_2ase system is comparable to that of the previously reported system using *Dmb* [NiFeSe]-H_2ase and graphitic carbon nitride as a photosensitizer where a TOF_{H2ase} of 5.5 × 10^3 and TON_{H2ase} of 50 × 10^3 after 48 h were reported.[32]

Negligible H_2 production was observed in the dark or in the absence of CDs, H_2ase, or EDTA (Table S1, Figures 5 and S8). Photo-H_2 production activity ceased when the sample was irradiated at 25 °C after heating to 100 °C for 15 min, i.e., conditions which denature the enzyme (Figure S9). These control experiments together indicate that H_2 production indeed arises from H_2ase following photoexcited electron transfer from CD-$NHMe_2^+$. Addition of free DMEN to the CD-CO_2^--H_2ase system does not give rise to H_2 production activity (Figure S9), demonstrating that the surface-bound amine is required for the high activity in the system (see below).

The light intensity was varied to gain further insight into the performance limiting factors of the CD-$NHMe_2^+$-H_2ase system. Cutting the light intensity by 50% and 80% using neutral density filters resulted in a linear decrease in the TOF_{H2ase}, indicating that the system is limited by light intensity (Figure S10, Table S3). The external quantum efficiency (EQE) was measured by irradiation of the samples using a monochromatic light source at an excitation wavelength of 365 nm with an intensity of 1.18 mW cm^{-2}. The resulting EQE of 0.36 ± 0.02% is an order of magnitude higher than a carbon nitride-H_2ase system (0.07%; λ = 360 nm)[32] and is comparable to a carbon nitride sensitized TiO_2 system under visible light irradiation (0.51%; λ = 400 nm).[31] Other visible light responsive, precious and toxic element-free systems cannot compete with the CD-$NHMe_2^+$-H_2ase system in terms of stability.[26]

CD−Enzyme Interface. Previous studies with immobilized H_2ases have highlighted key features required to achieve efficient nonmediated interfacial electron transfer.[17,48,70] Important parameters are the distance and orientation of the biocatalyst to the photosensitizer surface.[70] For example, strong electrostatic interactions were utilized to achieve high electron transfer efficiency between positively charged CdTe particles and the negatively charged carboxylate residues at the distal FeS cluster of a [NiFe]-H_2ase from *Thiocapsa roseopersicina*.[34] Similarly, a positively charged [FeFe]-H_2ase from *Clostridium acetobutylicum* has been integrated with negatively charged CdS and CdTe particles.[33,35]

In order to establish whether the markedly different activity between the anionic and cationic CDs here can be explained by different electrostatic interactions with the enzymes, we conducted photocatalytic experiments in the presence of a soluble redox mediator, methyl viologen (MV^{2+}; $E^{\circ\prime}$ = −0.45 V vs SHE).[81] A comparison of product formation in the presence and absence of MV^{2+} provides an indication of the efficiency of the direct electron transfer between the CD and enzyme and, in turn, is a measure of the interfacial interaction between them.

Product formation with both FccA and H_2ase is greatly enhanced for both types of CD in the presence of excess MV^{2+} (Table 1, Figures S11 and S12). For the H_2ase system, addition of MV^{2+} enhances the CD-$NHMe_2^+$ TOF_{H2ase} by a factor of 6 (Table 1). While this indicates that the CD-H_2ase interaction is not fully optimized, the interaction compares well with previously reported benchmark systems. A CN_x−H_2ase[32] system displayed a 22-fold enhancement on addition of MV^{2+}, and CN_x/TiO_2−H_2ase showed a 5-fold enhancement.[31] CD-$NHMe_2^+$ also exhibits a good interfacial interaction with FccA, with only a factor of 2 enhancement in substrate turnover in the presence of MV^{2+}. Control experiments irradiating CDs and MV^{2+} in the absence of H_2ase produced negligible H_2.

The photocatalytic experiments with MV^{2+} also highlight the stability of the CDs for sustaining enzyme-driven catalysis for up to 3 days, which is consistent with the previously reported photostability of CDs with synthetic catalysts.[56] In the presence of MV^{2+} solar H_2 production was sustained from the CD-H_2ase systems for over 72 h, reaching a TON_{H2ase} of 4.9 × 10^5 for

DOI: 10.1021/jacs.6b10146
J. Am. Chem. Soc. XXXX, XXX, XXX−XXX

Table 1. Summary of the Photocatalytic Performance of the CD−Enzyme Systems under Standard Conditions in the Presence or Absence of MV^{2+} [a]

	$TOF_{enzyme} \pm \sigma/10^3\ h^{-1}$	
	CD-CO_2^-	CD-$NHMe_2^+$
FccA	nd[b]	1.7 ± 0.4
FccA + MV^{2+}	3.0 ± 0.4	3.4 ± 1.2
H_2ase	0.3 ± 0.1	3.9 ± 0.9
H_2ase + MV^{2+}	26 ± 6	24 ± 7

[a]Conditions: Simulated solar irradiation (AM 1.5G, 1 sun) at 25 °C. For FccA: CDs (1 mg), FccA (0.22 nmol), fumarate (10 mM), MV^{2+} (0.2 mmol), and EDTA (0.1 M) in D_2O (pD 6.4), total solution volume 1 mL. For H_2ase: CDs (10 mg), H_2ase (50 pmol), MV^{2+} (5 μmol), in aqueous EDTA (0.1 M, pH 6), total solution volume 3 mL. [b]No succinate detected by ^1H NMR spectroscopy after 2 h irradiation.

CD-CO_2^- and 7.2×10^5 for CD-$NHMe_2^+$, respectively (Figure S11, Table S1). This long-term activity indicates that the loss of photocatalytic activity over time observed in the absence of MV^{2+} (Figures 2 and 4) is due to degradation of the enzymes rather than the CD, consistent with previous photocatalytic studies utilizing H_2ase and FccA.[32,44]

An important observation is that, in the presence of MV^{2+}, the enzyme-based TOFs for CD-CO_2^- and CD-$NHMe_2^+$ are almost identical (Table 1, Figures S11 and S12). This implies that both enzymes are similarly active in both CD solutions under illumination and that any electrostatic interactions with the enzymes do not affect the intrinsic enzyme activity.[57] It also demonstrates that the driving force and kinetics for MV^{2+} reduction and EDTA oxidation are comparable for both types of CDs. The striking difference in performance between the two CDs in these systems in the absence of MV^{2+} can thus be attributed to the difference in CD surface charge and different interfacial interaction with the enzyme.

Figure 6 shows the ribbon representation based on X-ray crystal coordinates of FccA[75] and *Dmb* [NiFeSe]-H_2ase[82] with the surface-exposed positively and negatively charged amino acid residues highlighted. The surface-exposed electron entry sites (i.e., an Fe-heme subunit for FccA and $[Fe_4S_4]$-cluster for H_2ase) are surrounded by negatively charged aspartate and glutamate residues in both enzymes, as well as carboxylate groups on the surface-exposed hemes in FccA. Furthermore, the I_p of *Dmb* [NiFeSe]-H_2ase has been reported to be at pH 5.4[48] and the enzyme is therefore predominantly negatively charged under the experimental conditions employed in this study. The high photocatalytic performance with CD-$NHMe_2^+$ is thus consistent with a favorable electrostatic interaction with the enzymes and in particular with the concentrated negatively charged residues at the electron entry sites, allowing for efficient direct electron transfer. Similarly, a poor interaction with the enzymes can be expected with negatively charged CD-CO_2^- consistent with its poor photocatalytic performance in the absence of MV^{2+}.

CONCLUSIONS

CDs are established as efficient photosensitizers for light-driven catalysis with redox enzymes, combining the benefits of molecular dyes, such as good solubility in water, with the high stability of semiconductor nanoparticles. Photocatalytic H_2 generation with H_2ase and light-driven C=C bond hydrogenation with FccA have been demonstrated by taking advantage of the tunable surface chemistry of the CDs.

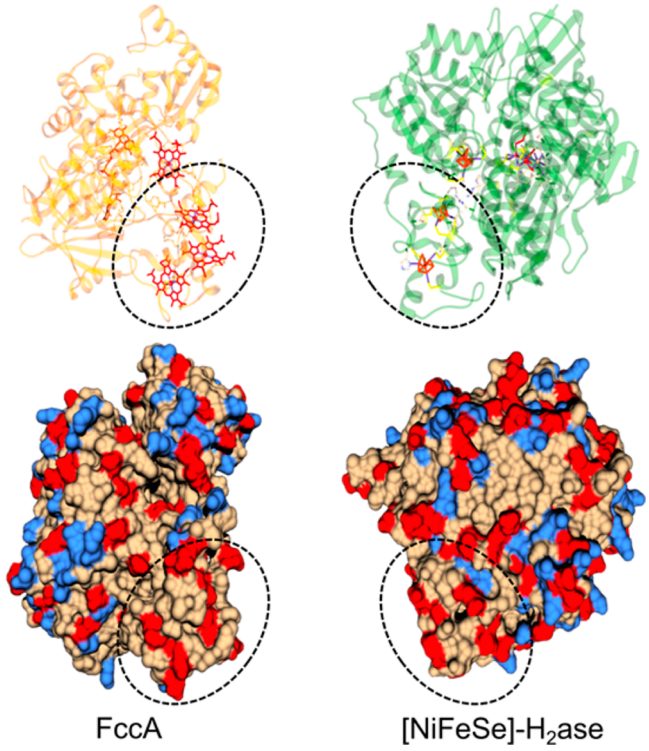

Figure 6. Ribbon and surface-charge representations of FccA and *Dmb* [NiFeSe]-H_2ase based on X-ray crystal structures (PDB codes 1D4C and 1CC1 for FccA[75] and H_2ase,[82] respectively). The location of the Fe-heme and $[Fe_4S_4]$ cofactors responsible for interfacial electron exchange are highlighted. The bottom structures highlight the negative (red) and positive (blue) surface charges on the enzymes.

Positively charged ammonium-terminated CD-$NHMe_2^+$ display excellent interfacial interactions and efficient direct electron transfer to FccA and H_2ase, whereas negatively charged CDs show little or no activity. Direct photoexcited electron transfer to FccA was observed spectroscopically, and solar-driven fumarate to succinate conversion over 24 h was confirmed. CD-$NHMe_2^+$ also displayed long-term solar H_2 production with H_2ase and compares well with previously reported systems.

Ample opportunities for enhancement of the overall performance are available, for example, through optimization of the intrinsic CD properties (e.g., via graphitization or heteroatom doping)[83,84] or by covalent immobilization of the enzyme.[27] The tunable surface chemistry of CDs along with their properties of aqueous solubility, biocompatibility, and high stability render CDs as versatile photosensitizers for biohybrid photocatalytic schemes and will also allow their use for fundamental studies of electron transfer in CD−biomolecule assemblies.[85,86]

EXPERIMENTAL SECTION

Materials. Reagents used throughout this work were obtained from commercial suppliers and used as received unless otherwise stated. Laboratory grade reagents were used in all synthetic procedures and chemicals for the analytical part of the work were of the highest available purity. Millipore water (18.2 MΩ cm at 25 °C) was used throughout this work in both synthetic and analytical procedures. Buffer solutions were made using analytical grade reagents and titrated to the desired pH, as determined by a pH electrode (Mettler Toledo; SevenEasy) using NaOH. D_2O titrations were carried out with NaOD using an electrode calibrated in aqueous solution, and a correction

DOI: 10.1021/jacs.6b10146
J. Am. Chem. Soc. XXXX, XXX, XXX−XXX

factor of 0.4 was applied to convert the pH meter reading to pD.[77] DMEN (Aldrich, ≥ 98%) was dried over activated molecular sieves (4 Å) prior to use.

Enzymes. *Dmb* [NiFeSe]-H_2ase was purified following a previously reported procedure.[87] The preparation has a specific activity of 2115 μmol H_2 min^{-1} (mg H_2ase)$^{-1}$.[88] FccA from *Shewanella oneidensis* MR-1 was purified using a previously reported procedure.[89] The purified sample coupled oxidation of dithionite-reduced methyl viologen to fumarate reduction at a rate of 18.3 mM succinate min^{-1} (mg FccA)$^{-1}$.

Synthesis of CDs. CD-CO_2^- was synthesized and characterized as previously described.[55,71] Briefly, citric acid (100 g) was thermolyzed under air at 180 °C for 40 h producing carboxylic acid capped amorphous CDs as an orange-brown high-viscosity liquid. The CDs were dissolved in water and freeze-dried to yield CD-CO_2H as a yellow-orange powder. To obtain sodium carboxylate capped CDs (CD-CO_2^-), the CD solution was neutralized to pH 7 using aqueous NaOH solution (5 M) prior to freeze-drying. Carboxylic acid capped CDs (CD-CO_2H) were used for the synthesis of CD-NMe_2, and sodium carboxylate capped CDs (CD-CO_2^-) were used for the photocatalysis experiments. For CD-$CO_2^-Na^+$, microanalysis found: C, 37.93%; H, 3.45%; N, 0.00%.

CD-COCl was prepared by refluxing CD-CO_2H (1.10 g) in neat thionyl chloride (50 mL) at 80 °C under a N_2 atmosphere for 1 h. Thionyl chloride was removed under reduced pressure, and the resulting CD-COCl were dissolved in dry tetrahydrofuran (5 mL) and filtered. The solvent was evaporated under high vacuum to yield acyl chloride capped CDs (CD-COCl, 1.0 g). Microanalysis found: C, 54.95%; H, 3.5%; Cl, 11.19%; N, 0.00%.

CD-NMe_2 was prepared by stirring CD-COCl (800 mg) with neat dry DMEN (25 mL) at room temperature in the dark for 3 h, whereupon DMEN was removed under high vacuum. The CD-NMe_2 were dissolved in acetone and filtered through a 0.2 μm syringe filter. Acetone was removed under reduced pressure and the product redispersed in methanol and the solvent removed (3 × 5 mL) before drying for 12 h under high vacuum at 40 °C. The resulting CD-NMe_2 were then dissolved in water and freeze-dried to yield a light brown hygroscopic solid. Microanalysis found: C, 57.75%; H, 8.8%; Cl, 4.92%, N, 14.75%. Prior to use in photocatalytic experiments a stock solution of CD-$NHMe_2^+$ was prepared (50 mg mL^{-1} in 0.1 M EDTA, pH 6).

Physical Characterization Techniques. TEM images were collected on a FEI Technai F20 FEG S/TEM operating at 200 kV. ATR FT-IR was carried out on a Thermo Scientific Nicolet iS50 FT-IR spectrometer. ^{1}H NMR spectra were taken using a Bruker 400 MHz spectrometer. UV−visible spectroscopy was carried out on a Varian Cary 50 UV−vis spectrophotometer using quartz cuvettes with 1 cm path length. Zeta potential measurements were carried out on a Malvern Zetasizer Nano ZS. Elemental analyses were carried out by the microanalytical laboratory in the Department of Chemistry, University of Cambridge; the CD-COCl and CD-NMe_2 analyses were carried out in airtight capsules prepared in an anhydrous glovebox to avoid moisture contamination.

Photocatalysis Experiments. All photocatalysis experiments were carried out in borosilicate glass vessels placed in a thermoregulated water bath at 25 °C with stirring. Vials were irradiated using a regularly calibrated solar light simulator (Newport Oriel) under full spectrum (λ > 300 nm) AM 1.5G irradiation at an intensity of 100 mW cm^{-2}, unless otherwise stated.

Photocatalysis Experiments with FccA. Photocatalytic experiments were set up by dissolving CDs (1 mg), FccA (0.22 nmol), and fumarate (10 mM) in an EDTA solution (0.1 M) prepared in D_2O (99.99%; pD 6.4). The total solution volume was 1 mL. FccA was added from a stock solution (11 μM) in aqueous MES buffer (25 mM, pH 6.5). The vials were sealed with a septum (Suba-Seal) and purged with N_2 prior to irradiation. Aliquots of the photocatalysis mixture (0.2 mL) were taken and analyzed directly by ^{1}H NMR spectroscopy (400 MHz, Bruker). The TON_{FccA} for succinate was determined by the integral ratio of the peaks corresponding to fumarate (6.44 ppm) and succinate (2.33 ppm).[44] Since the experiments were performed in D_2O, the product of the enzymatic reaction will be predominantly succinate with 2 aliphatic protons and 2 aliphatic deuterons.

Photocatalysis Experiments with H_2ase. Photocatalytic experiments were set up in an anaerobic glovebox by combining degassed aqueous solutions containing CDs (typically 10 mg) and EDTA (0.1 M, pH 6). H_2ase was added from a stock solution (3 μM) in aqueous TEOA buffer (0.1 M, pH 7), which was stored frozen in the glovebox. The total volume of the photoreactor was 7.74 mL and the solution volume 3 mL. The vessels were sealed with a septum, removed from the glovebox, and purged with N_2 containing 2% CH_4 as a GC standard for at least 10 min prior to irradiation. H_2 detection was carried out by GC (Agilent 7890A) with a 5 Å molecular sieve column and a thermal conductivity detector. The GC oven was held at 45 °C and N_2 was used as the carrier gas (flow rate 3 mL min^{-1}). Aliquots of headspace gas (50 μL) were removed from the reaction vessel using a gastight syringe (Hamilton; GASTIGHT). H_2 produced was quantified by comparison to the CH_4 internal standard. The gas chromatograph was calibrated regularly to ensure reproducibility.

Treatment of Data. All analytical measurements were performed in triplicate. The data were treated as follows: for a sample of n observations x_i, the unweighted mean value x_0 and the standard deviation σ were calculated using the equations:

$$x_0 = \sum_i \frac{x_i}{n} \qquad \sigma = \sqrt{\frac{\sum_i (x_i - x_0)^2}{n-1}}$$

A minimum σ of 10% was assumed. TOF and TON with respect to the enzymes are expressed in the units $(mol_{product})$ $(mol_{enzyme})^{-1}$ h^{-1} and $(mol_{product})$ $(mol_{enzyme})^{-1}$, respectively. TOF_{H2ase} and TOF_{FccA} were calculated from product formation after 1 and 2 h illumination, respectively. Unless otherwise stated, the TON_{H2ase} and TON_{FccA} are reported after 24 h irradiation.

External Quantum Efficiency (EQE) Measurement. H_2 production was carried out in an airtight quartz cuvette with stirring (3.89 mL total volume, 2 mL solution volume). The vial was irradiated for 24 h over a fixed area (1 cm^2) with a Xe lamp (LOT) equipped with a monochromator (LOT MSH300) set to λ = 365 nm with a full width at half-maximum of 15 nm. The light intensity was measured using an International Light Technologies photometer (ILT1400); I = 1.18 mW cm^{-2}. The EQE was calculated using the following formula:

$$\text{EQE}\ (\%) = \frac{(2n_{H2}N_A hc)}{(t_{irr}\lambda IA)} \times 100$$

where n_{H2} is the number of moles of photogenerated hydrogen, t_{irr} is the irradiation time (s), A is irradiation cross section (m^2), and N_A, h, and c are Avogadro's constant (mol^{-1}), the Planck constant (m^2 kg s^{-1}), and the speed of light (m s^{-1}), respectively.

■ ASSOCIATED CONTENT

Supporting Information

The Supporting Information is available free of charge on the ACS Publications website at DOI: 10.1021/jacs.6b10146.

Supporting Tables and Figures: ^{1}H NMR and UV−vis spectra, TEM image, zeta potential plot, and solar H_2 and succinate production (PDF). Additional data related to this publication are available at the University of Cambridge data repository (http://dx.doi.org/10.17863/CAM.6573).

■ AUTHOR INFORMATION

Corresponding Author

*reisner@ch.cam.ac.uk

ORCID

Erwin Reisner: 0000-0002-7781-1616

DOI: 10.1021/jacs.6b10146
J. Am. Chem. Soc. XXXX, XXX, XXX−XXX

Present Address

[§]Department of Chemistry, University of New Hampshire, 23 Academic Way, Durham, NH, 03824, USA.

Notes

The authors declare no competing financial interest.

■ ACKNOWLEDGMENTS

This work was supported by a Cambridge Australia Poynton PhD scholarship (to G.A.M.H.), the BBSRC (BB/K010220/1 to E.R. and BB/K009885/1 to J.N.B.), an Oppenheimer PhD scholarship (to B.C.M.M.), and a Marie Curie postdoctoral fellowship (GAN 624997 to C.A.C.). We thank Dr. J. C. Fontecilla-Camps and Dr. C. Cavazza (CNRS Grenoble, France) for providing us with *Dmb* [NiFeSe]-H_2ase. Dr. Lars Jeuken, Dr. Jenny Zhang, David Wakerley, and Janina Willkomm are thanked for helpful discussions or comments on the manuscript.

■ REFERENCES

(1) Tachibana, Y.; Vayssieres, L.; Durrant, J. R. *Nat. Photonics* **2012**, *6*, 511−518.
(2) Gust, D.; Moore, T. A. *Science* **1989**, *244*, 35−41.
(3) Magnuson, A.; Anderlund, M.; Johansson, O.; Lindblad, P.; Lomoth, R.; Polivka, T.; Ott, S.; Stensjö, K.; Styring, S.; Sundström, V.; Hammarström, L. *Acc. Chem. Res.* **2009**, *42*, 1899−1909.
(4) Woolerton, T. W.; Sheard, S.; Pierce, E.; Ragsdale, S. W.; Armstrong, F. A. *Energy Environ. Sci.* **2011**, *4*, 2393−2399.
(5) Brown, K. A.; Harris, D. F.; Wilker, M. B.; Rasmussen, A.; Khadka, N.; Hamby, H.; Keable, S.; Dukovic, G.; Peters, J. W.; Seefeldt, L. C.; King, P. W. *Science* **2016**, *352*, 448−450.
(6) Lee, C.-Y.; Park, H. S.; Fontecilla-Camps, J. C.; Reisner, E. *Angew. Chem., Int. Ed.* **2016**, *55*, 5971−5974.
(7) Roth, L. E.; Nguyen, J. C.; Tezcan, F. A. *J. Am. Chem. Soc.* **2010**, *132*, 13672−13674.
(8) Zhao, Y.; Anderson, N. C.; Ratzloff, M. W.; Mulder, D. W.; Zhu, K.; Turner, J. A.; Neale, N. R.; King, P. W.; Branz, H. M. *ACS Appl. Mater. Interfaces* **2016**, *8*, 14481−14487.
(9) Nichols, E. M.; Gallagher, J. J.; Liu, C.; Su, Y.; Resasco, J.; Yu, Y.; Sun, Y.; Yang, P.; Chang, M. C. Y.; Chang, C. J. *Proc. Natl. Acad. Sci. U. S. A.* **2015**, *112*, 11461−11466.
(10) Torella, J. P.; Gagliardi, C. J.; Chen, J. S.; Bediako, D. K.; Colón, B.; Way, J. C.; Silver, P. A.; Nocera, D. G. *Proc. Natl. Acad. Sci. U. S. A.* **2015**, *112*, 2337−2343.
(11) Park, J. H.; Lee, S. H.; Cha, G. S.; Choi, D. S.; Nam, D. H.; Lee, J. H.; Lee, J.-K.; Yun, C.-H.; Jeong, K. J.; Park, C. B. *Angew. Chem., Int. Ed.* **2015**, *54*, 969−973.
(12) Liu, C.; Colón, B. C.; Ziesack, M.; Silver, P. A.; Nocera, D. G. *Science* **2016**, *352*, 1210−1213.
(13) Sakimoto, K. K.; Wong, A. B.; Yang, P. *Science* **2016**, *351*, 74−77.
(14) Hambourger, M.; Gervaldo, M.; Svedruzic, D.; King, P. W.; Gust, D.; Ghirardi, M.; Moore, A. L.; Moore, T. A. *J. Am. Chem. Soc.* **2008**, *130*, 2015−2022.
(15) Mersch, D.; Lee, C.-Y.; Zhang, J. Z.; Brinkert, K.; Fontecilla-Camps, J. C.; Rutherford, A. W.; Reisner, E. *J. Am. Chem. Soc.* **2015**, *137*, 8541−8549.
(16) Woolerton, T. W.; Sheard, S.; Chaudhary, Y. S.; Armstrong, F. A. *Energy Environ. Sci.* **2012**, *5*, 7470−7490.
(17) Rüdiger, O.; Abad, J. M.; Hatchikian, E. C.; Fernandez, V. M.; De Lacey, A. L. *J. Am. Chem. Soc.* **2005**, *127*, 16008−16009.
(18) Kato, M.; Cardona, T.; Rutherford, A. W.; Reisner, E. *J. Am. Chem. Soc.* **2013**, *135*, 10610−10613.
(19) Vincent, K. A.; Parkin, A.; Armstrong, F. A. *Chem. Rev.* **2007**, *107*, 4366−4413.
(20) Lubitz, W.; Ogata, H.; Rüdiger, O.; Reijerse, E. *Chem. Rev.* **2014**, *114*, 4081−4148.
(21) Jones, A. K.; Sillery, E.; Albracht, S. P. J.; Armstrong, F. A. *Chem. Commun.* **2002**, 866−867.
(22) Okura, I. *Coord. Chem. Rev.* **1985**, *68*, 53−99.
(23) Krassen, H.; Schwarze, A.; Friedrich, B.; Ataka, K.; Lenz, O.; Heberle, J. *ACS Nano* **2009**, *3*, 4055−4061.
(24) Lubner, C. E.; Knörzer, P.; Silva, P. J. N.; Vincent, K. A.; Happe, T.; Bryant, D. A.; Golbeck, J. H. *Biochemistry* **2010**, *49*, 10264−10266.
(25) Tapia, C.; Milton, R. D.; Pankratova, G.; Minteer, S. D.; Åkerlund, H.-E.; Leech, D.; De Lacey, A. L.; Pita, M.; Gorton, L. *ChemElectroChem* **2016**, DOI: 10.1002/celc.201600506.
(26) Sakai, T.; Mersch, D.; Reisner, E. *Angew. Chem., Int. Ed.* **2013**, *52*, 12313−12316.
(27) Zadvornyy, O. A.; Lucon, J. E.; Gerlach, R.; Zorin, N. A.; Douglas, T.; Elgren, T. E.; Peters, J. W. *J. Inorg. Biochem.* **2012**, *106*, 151−155.
(28) Noji, T.; Kondo, M.; Jin, T.; Yazawa, T.; Osuka, H.; Higuchi, Y.; Nango, M.; Itoh, S.; Dewa, T. *J. Phys. Chem. Lett.* **2014**, *5*, 2402−2407.
(29) Lam, Q.; Kato, M.; Cheruzel, L. *Biochim. Biophys. Acta, Bioenerg.* **2016**, *1857*, 589−597.
(30) Reisner, E.; Fontecilla-Camps, J. C.; Armstrong, F. A. *Chem. Commun.* **2009**, 550−552.
(31) Caputo, C. A.; Wang, L.; Beranek, R.; Reisner, E. *Chem. Sci.* **2015**, *6*, 5690−5694.
(32) Caputo, C. A.; Gross, M. A.; Lau, V. W.; Cavazza, C.; Lotsch, B. V.; Reisner, E. *Angew. Chem., Int. Ed.* **2014**, *53*, 11538−11542.
(33) Wilker, M. B.; Shinopoulos, K. E.; Brown, K. A.; Mulder, D. W.; King, P. W.; Dukovic, G. *J. Am. Chem. Soc.* **2014**, *136*, 4316−4324.
(34) Greene, B. L.; Joseph, C. A.; Maroney, M. J.; Dyer, R. B. *J. Am. Chem. Soc.* **2012**, *134*, 11108−11111.
(35) Brown, K. A.; Dayal, S.; Ai, X.; Rumbles, G.; King, P. W. *J. Am. Chem. Soc.* **2010**, *132*, 9672−9680.
(36) Tapia, C.; Zacarias, S.; Pereira, A. C. I.; Conesa, J. C.; Pita, M.; De Lacey, A. L. *ACS Catal.* **2016**, *6*, 5691−5698.
(37) Schmid, A.; Dordick, J. S.; Hauer, B.; Kiener, A.; Wubbolts, M.; Witholt, B. *Nature* **2001**, *409*, 258−268.
(38) Lee, S. H.; Kim, J. H.; Park, C. B. *Chem. - Eur. J.* **2013**, *19*, 4392−4406.
(39) Lewis, J. C.; Arnold, F. H. *Chimia* **2009**, *63*, 309−312.
(40) Taglieber, A.; Schulz, F.; Hollmann, F.; Rusek, M.; Reetz, M. T. *ChemBioChem* **2008**, *9*, 565−572.
(41) Reeve, H. A.; Lauterbach, L.; Lenz, O.; Vincent, K. A. *ChemCatChem* **2015**, *7*, 3480−3487.
(42) Maciá-Agulló, J. A.; Corma, A.; Garcia, H. *Chem. - Eur. J.* **2015**, *21*, 10940−10959.
(43) Köninger, K.; Baraibar, Á. G.; Mügge, C.; Paul, C. E.; Hollmann, F.; Nowaczyk, M. M.; Kourist, R. *Angew. Chem., Int. Ed.* **2016**, *55*, 5582−5585.
(44) Bachmeier, A.; Murphy, B. J.; Armstrong, F. A. *J. Am. Chem. Soc.* **2014**, *136*, 12876−12879.
(45) Kato, M.; Nguyen, D.; Gonzalez, M.; Cortez, A.; Mullen, S. E.; Cheruzel, L. E. *Bioorg. Med. Chem.* **2014**, *22*, 5687−5691.
(46) Winkler, J. R.; Gray, H. B. *Chem. Rev.* **1992**, *92*, 369−379.
(47) Hall, D. B.; Holmlin, R. E.; Barton, J. K. *Nature* **1996**, *382*, 731−735.
(48) Reisner, E.; Powell, D. J.; Cavazza, C.; Fontecilla-Camps, J. C.; Armstrong, F. A. *J. Am. Chem. Soc.* **2009**, *131*, 18457−18466.
(49) Brown, K. A.; Wilker, M. B.; Boehm, M.; Dukovic, G.; King, P. W. *J. Am. Chem. Soc.* **2012**, *134*, 5627−5636.
(50) Dobbin, P. S.; Butt, J. N.; Powell, A. K.; Reid, G. A.; Richardson, D. J. *Biochem. J.* **1999**, *342*, 439−448.
(51) Morris, C. J.; Black, A. C.; Pealing, S. L.; Manson, F. D. C.; Chapman, S. K.; Reid, G. A.; Gibson, D. M.; Ward, F. B. *Biochem. J.* **1994**, *302*, 587−593.
(52) Cayuela, A.; Soriano, M. L.; Carrillo-Carrión, C.; Valcárcel, M. *Chem. Commun.* **2016**, *52*, 1311−1326.
(53) Baker, S. N.; Baker, G. A. *Angew. Chem., Int. Ed.* **2010**, *49*, 6726−6744.
(54) Li, H.; Kang, Z.; Liu, Y.; Lee, S.-T. *J. Mater. Chem.* **2012**, *22*, 24230.

DOI: 10.1021/jacs.6b10146
J. Am. Chem. Soc. XXXX, XXX, XXX−XXX

(55) Martindale, B. C. M.; Hutton, G. A. M.; Caputo, C. A.; Reisner, E. *J. Am. Chem. Soc.* **2015**, *137*, 6018−6025.
(56) Martindale, B. C. M.; Joliat, E.; Bachmann, C.; Alberto, R.; Reisner, E. *Angew. Chem., Int. Ed.* **2016**, *55*, 9402−9406.
(57) Essner, J. B.; McCay, R. N.; Smith, C. J., II; Cobb, S. M.; Laber, C. H.; Baker, G. A. *J. Mater. Chem. B* **2016**, *4*, 2163−2170.
(58) Das, K.; Maiti, S.; Das, P. K. *Langmuir* **2014**, *30*, 2448−2459.
(59) Hou, J.; Dong, J.; Zhu, H.; Teng, X.; Ai, S.; Mang, M. *Biosens. Bioelectron.* **2015**, *68*, 20−26.
(60) Li, H.; Guo, S.; Li, C.; Huang, H.; Liu, Y.; Kang, Z. *ACS Appl. Mater. Interfaces* **2015**, *7*, 10004−10012.
(61) Li, H.; Kong, W.; Liu, J.; Yang, M.; Huang, H.; Liu, Y.; Kang, Z. *J. Mater. Chem. B* **2014**, *2*, 5652−5658.
(62) Rasmussen, M.; Wingersky, A.; Minteer, S. D. *ECS Electrochem. Lett.* **2014**, *3*, H1−H3.
(63) Ge, J.; Jia, Q.; Liu, W.; Guo, L.; Liu, Q.; Lan, M.; Zhang, H.; Meng, X.; Wang, P. *Adv. Mater.* **2015**, *27*, 4169−4177.
(64) Zheng, M.; Liu, S.; Li, J.; Qu, D.; Zhao, H.; Guan, X.; Hu, X.; Xie, Z.; Jing, X.; Sun, Z. *Adv. Mater.* **2014**, *26*, 3554−3560.
(65) Yang, S.-T.; Wang, X.; Wang, H.; Lu, F.; Luo, P. G.; Cao, L.; Meziani, M. J.; Liu, J.-H.; Liu, Y.; Chen, M.; Huang, Y.; Sun, Y.-P. *J. Phys. Chem. C* **2009**, *113*, 18110−18114.
(66) Ray, S. C.; Saha, A.; Jana, N. R.; Sarkar, R. *J. Phys. Chem. C* **2009**, *113*, 18546−18551.
(67) Li, H.; Zhang, Y.; Wang, L.; Tian, J.; Sun, X. *Chem. Commun.* **2011**, *47*, 961−963.
(68) Wang, Y.; Lu, L.; Peng, H.; Xu, J.; Wang, F.; Qi, R.; Xu, Z.; Zhang, W. *Chem. Commun.* **2016**, *52*, 9247−9250.
(69) Maiti, S.; Das, K.; Das, P. K. *Chem. Commun.* **2013**, *49*, 8851−8853.
(70) King, P. W. *Biochim. Biophys. Acta, Bioenerg.* **2013**, *1827*, 949−952.
(71) Guo, C. X.; Zhao, D.; Zhao, Q.; Wang, P.; Lu, X. *Chem. Commun.* **2014**, *50*, 7318−7321.
(72) Wang, X.; Cao, L.; Yang, S.-T.; Lu, F.; Meziani, M. J.; Tian, L.; Sun, K. W.; Bloodgood, M. A.; Sun, Y.-P. *Angew. Chem., Int. Ed.* **2010**, *49*, 5310−5314.
(73) Liu, C.; Bao, L.; Tang, B.; Zhao, J.-Y.; Zhang, Z.-L.; Xiong, L.-H.; Hu, J.; Wu, L.-L.; Pang, D.-W. *Small* **2016**, *12*, 4702−4706.
(74) Turner, K. L.; Doherty, M. K.; Heering, H. A.; Armstrong, F. A.; Reid, G. A.; Chapman, S. K. *Biochemistry* **1999**, *38*, 3302−3309.
(75) Leys, D.; Tsapin, A. S.; Nealson, K. H.; Meyer, T. E.; Cusanovich, M. A.; Van Beeumen, J. J. *Nat. Struct. Biol.* **1999**, *6*, 1113−1117.
(76) Doherty, M. K.; Pealing, S. L.; Miles, C. S.; Moysey, R.; Taylor, P.; Walkinshaw, M. D.; Reid, G. A.; Chapman, S. K. *Biochemistry* **2000**, *39*, 10695−10701.
(77) Glasoe, P. K.; Long, F. A. *J. Phys. Chem.* **1960**, *64*, 188−190.
(78) Wombwell, C.; Caputo, C. A.; Reisner, E. *Acc. Chem. Res.* **2015**, *48*, 2858−2865.
(79) Baltazar, C. S. A.; Marques, M. C.; Soares, C. M.; DeLacey, A. M.; Pereira, I. A. C.; Matias, P. M. *Eur. J. Inorg. Chem.* **2011**, 948−962.
(80) Parkin, A.; Goldet, G.; Cavazza, C.; Fontecilla-Camps, J. C.; Armstrong, F. A. *J. Am. Chem. Soc.* **2008**, *130*, 13410−13416.
(81) Bird, C. L.; Kuhn, A. T. *Chem. Soc. Rev.* **1981**, *10*, 49−82.
(82) Garcin, E.; Vernede, X.; Hatchikian, E. C.; Volbeda, A.; Frey, M.; Fontecilla-Camps, J. C. *Structure* **1999**, *7*, 557−566.
(83) Jiang, K.; Sun, S.; Zhang, L.; Lu, Y.; Wu, A.; Cai, C.; Lin, H. *Angew. Chem., Int. Ed.* **2015**, *54*, 5360−5363.
(84) Moon, B. J.; Oh, Y.; Shin, D. H.; Kim, S. J.; Lee, S. H.; Kim, T.-W. W.; Park, M.; Bae, S. *Chem. Mater.* **2016**, *28*, 1481−1488.
(85) Arnold, A. R.; Grodick, M. A.; Barton, J. K. *Cell Chem. Biol.* **2016**, *23*, 183−197.
(86) Winkler, J. R.; Gray, H. B. *Chem. Rev.* **2014**, *114*, 3369−3380.
(87) Volbeda, A.; Amara, P.; Iannello, M.; De Lacey, A. L.; Cavazza, C.; Fontecilla-Camps, J. C. *Chem. Commun.* **2013**, *49*, 7061−7063.
(88) Hatchikian, E. C.; Bruschi, M.; Le Gall, J. *Biochem. Biophys. Res. Commun.* **1978**, *82*, 451−461.
(89) Lee, C.-Y.; Reuillard, B.; Sokol, K. P.; Laftsoglou, T.; Lockwood, C. W. J.; Rowe, S. F.; Hwang, E. T.; Fontecilla-Camps, J.-C.; Jeuken, L. J. C.; Butt, J. N.; Reisner, E. *Chem. Commun.* **2016**, *52*, 7390−7393.

DOI: 10.1021/jacs.6b10146
J. Am. Chem. Soc. XXXX, XXX, XXX−XXX